PACS numbers: 42.55.Lt; 42.60.Lh
DOI: 10.1070/QE2002v032n05ABEH002217

Effect of molecular additions on the radiation parameters of a laser on Xe atomic transitions

A.V. Fedenev, V.F. Tarasenko, V.S. Skakun

***Abstract*. An electron-beam-pumped laser on Xe atomic transitions is experimentally investigated at various pump durations and powers within wide ranges of pressures and working mixtures including additions of molecular gases. It is shown that the maximum specific lasing powers are achieved at high specific pump powers (above 200 kW cm^{-3} atm^{-1}) and durations of the beam current pulse of tens of nanoseconds in high-pressure Ar–Xe mixtures with molecular gas additions (N_2 and CO_2). A specific output radiation power of $\sim$ 4 kW cm^{-3} is obtained. For a pump pulse durations from hundreds of nanoseconds to 1 μs, the highest lasing energies are reached without molecular additions at a comparatively low beam-current density (the specific pump power is $\sim$10 kW cm^{-3} atm^{-1}). However, in setups with specific pump powers above 40 kW cm^{-3} atm^{-1} and a working-mixture pressure limited by the strength of the laser chamber, molecular additions result in an increase in the radiation energy and efficiency. In wide-aperture facilities with high pump powers, molecular additions improve the distribution of the radiation power density over the laser-beam cross section.**

Keywords: *Xe laser, specific radiation power, electron-beam pumping*.

1. Introduction

Many papers (see [1–20] and references therein) are devoted to lasers on Xe atomic transitions. This is explained by the complexity of physical processes occurring in such lasers and by a variety of methods for their excitation. Laser radiation can be obtained at more than ten lines in the near IR region upon pumping by an electron beam, nuclear-reaction products, a self-sustained discharge, a discharge controlled or initiated by an electron beam, etc. However, the question of the influence of impurities or special additions of molecular gases on the lasing characteristics of a Xe laser has not been completely clarified up to now.

It was shown in [5, 12], that, at a high current density of the pump electron beam (10–100 A cm^{-2}), additions of molecular gases and helium make it possible to enhance the lasing power and energy. On the other hand, at low beam current densities, even comparatively small concentrations of molecular gas additions resulted in a reduction of the power and energy of the Xe laser radiation [8, 15, 20]. At a pump intensity of $\sim$ 40 W cm^{-2} and a concentration of air or CO_2 impurities above 0.01 %, an abrupt decrease in the laser radiation power was observed [15]. At a specific pump power of $\sim$ 0.4 kW cm^{-3} and nitrogen additions, a decrease in the radiation power was also observed [8].

It follows from the results of calculations performed in [20] that the lasing efficiency decreaes by $\sim$ 30 % at a specific pump power of $\sim$ 10 kW cm^{-3} atm^{-1}, if nitrogen and water impurities at a concentration of 0.05 % are present in an Ar–Xe mixture (at a pressure of 2–2.5 atm). The same concentration of impurities has no effect on the lasing energy and efficiency at a specific pump power of $\sim$ 30 kW cm^{-3} atm^{-1}. Note that, at a specific pump power of $\sim$ 30 kW cm^{-3} atm^{-1}, the radiation energies obtained by calculations and experimentally coincided. Moreover, the lasing energies obtained by calculations for a pure mixture and a mixture with a nitrogen and water impurity concentration of 0.05 % were also equal [20].

In this paper, we present the results of studies of a Xe atomic transition laser at various densities (0.005–100 A cm^{-2}) and durations (5 ns–100 μs) of the pump pulse beam current. The mixture pressure varied between 0.5 and 3.5 atm. Lasing was investigated in an Ar–Xe mixture doped with N_2 and CO_2 molecular gases.

2. Experimental

The experiments were carried out on four setups described in detail in papers [5, 7, 12–14]. Setup 1 [12] consisted of an electron accelerator with a planar vacuum diode (VD), which generated an electron beam with a size of 1 × 4 cm, and a laser chamber. The current density at the axis of the optical cavity was $\sim$ 50 A cm^{-2} at a current pulse full-width at half maximum (FWHM) $\tau_p \sim 3$ ns. The mean electron energy behind the foil was $\sim$ 140 keV.

Setup 2 [13] also consisted of an electron accelerator with a planar VD, which generated an electron beam with a cross section of 2 × 42 cm, and a laser chamber with a 0.2-L active volume. The current density behind the foil was 20–100 A cm^{-2} at $\tau_p \sim 60$ ns. The mean electron energy behind the foil was $\sim$ 150 keV.

In setup 3 [14], a coaxial plasma-cathode VD forming a radially converging electron beam was used, due to which a high pumping homogeneity over the laser-chamber (with a volume of 18 L, a diameter of 20 cm, and an active length of 60 cm) cross section was ensured at a pressure of 1–

A.V. Fedenev, V.F. Tarasenko, V.S. Skakun Institute of High-Current Electronics, Siberian Branch, Russian Academy of Sciences, pr. Akademicheskii 4, 634055 Tomsk, Russia; tel: (3822) 258 685; 259 392; fax: (3822) 259 410; e-mail: VFT@loi.hcei.tsc.ru

Received 19 February 2002
Kvantovaya Elektronika **32** (5) 449–454 (2002)
Translated by A.S. Seferov

1.5 atm. The current density at $\tau_p = 30 - 100$ μs was 0.1–0.005 A cm^{-2}, and the mean electron energy behind the foil was ~ 170 keV.

In setup 4 [21], on which the greater part of the data presented in this work was obtained, a coaxial plasma-cathode VD forming a radially converging electron beam was used as well. Due to this technique, a high pumping homogeneity over the laser-chamber (with a volume of 31 L, a diameter of 20 cm, and an active length of 100 cm) cross section was achieved. The current density in front of the foil was 5–40 A cm^{-2} for $\tau_p \sim 400$ ns. The mean electron energy behind the foil was a function of the charging voltage. When the charging voltage changed from 50 to 85 kV, the voltage across the VD changed from 300 to 500 kV. The total energy deposited to the gas in this setup was determined from the pressure jump [21].

Internal plane–parallel cavities consisting of a totally reflecting Al-coated mirror and output mirrors with reflectivities of 99, 95, 33, 27, and 6% at $\lambda = 1.73$ μm were employed in the experiments. The laser radiation energy was measured with an IMO-2N calorimeter and a PE-25 pyroelectric sensor. The shape of radiation pulses was recorded with an FSG-22-3A2 photoresistor, whose signal was fed to a TDS-3032 oscilloscope synchronously with a beam-current signal.

The working mixtures were prepared directly in laser chambers. According to certificates, the purity of gases was 99.998 % (Ar) and 99.9992 % (Xe). As is known, the purity of the initial gases, its maintenance in the course of experiments, and a homogeneous Xe distribution over the entire active volume are important conditions for the operation of a Xe atomic transition laser. When the electron beam interacts with the walls of the laser chamber and the foil, a desorption of the absorbed gases takes place, and the working mixture is contaminated with impurities.

On the other hand, after the working mixture of a wide-aperture laser is exchanged, its forced mixing and long-duration holding before the beginning of experiments are necessary. The mixing can be achieved after the stirring motor is switched on several times [11, 18], but it is difficult to monitor the presence of impurities evolved due to a gas desorption from the laser-chamber walls. Therefore, the measurements in the work were performed after several switch-ons of the stirring motor, when the radiation energy and its distribution over the laser-chamber cross section reached constant values.

Note that, after the mixture was mixed, the total lasing energy increased, but a small amount of uncontrolled impuritives could accumulate in the laser chamber. The lasing efficiencies are presented with respect to the energy deposited into the working mixture, which was measured from the pressure jump or calculated by the method described in [14].

3. Experimental results

The setups described above provided all basic regimes of pumping a laser based on an Ar–Xe mixture by an electron beam. This mixture was selected for investigations, because, when using Xe mixtures with other gases or pure Xe, the laser radiation energy was much lower.

Due to the short duration of the pump beam current in the setup 1, lasing appears after its termination. The maximum lasing energy was obtained in the Ar : Xe = 10 : 1 mixture at a 1.5-atm pressure. When ~ 1 % of N_2 was added to the Ar : Xe = 10 : 1 mixture, an increase in the radiation pulse power and duration (from 80 to 150 ns) was observed at 2.03 μm, and the lasing was quenched at 1.73 μm. The total lasing energy increased in this case. However, as the pressure rose up to 2.5 atm, an increase in the lasing energy at 2.03 μm with increasing nitrogen concentration was insignificant. When CO_2 molecules were added instead of N_2 at a pressure of 1.5 atm in the mixture, the lasing power at $\lambda = 2.03$ μm increased (by 30 % for CO_2 concentration of ~ 0.5 %) and the laser pulse width remained unaltered. CO_2 additions in an Ar–Xe mixture did not increase the lasing energy at a pressure of 2.5 atm. The main results obtained on setup 1 are given in [12].

At setup 2, lasing was initiated during the electron-beam action and the greater part of laser energy was emitted before the beam-current termination, although the radiation pulse width exceeded the beam-current duration by ~ 100 ns. The highest radiation energy was obtained at a 3-atm pressure, a component ratio Ar : Xe = 100 : 1, and a maximum beam-current density of 95 A cm^{-2} (a specific pump power was ~ 1 MW cm^{-3} atm^{-1}). Laser radiation was recordered at 2.65, 2.63, and 1.73 μm using a quartz plate served as the output mirror. The maximum radiation power was obtained at 2.65 μm. Higher pressures were not used in experiments because of a probable foil rupture.

The maximum positive effect of molecular additions was achieved on this setup. When N_2 or CO_2 additions were introduced to the mixture, an increase in the radiation power, energy, and, consequently, lasing efficiency by a factor of 2–3 was observed. Figure 1 shows plots of the specific radiation energy as a function of the Xe concentration in Ar–Xe–N_2 and Ar–Xe mixtures at a pressure of 2.5 atm. The maximum effect under the given conditions was achieved at a maximum beam-current density. An increase in the Xe concentration up to 4.8 % in mixtures with additions of molecular gases resulted in an increased radiation power. Molecular additions gave rise to the 2.03-μm line in the emission spectrum. In this case, the maximum lasing intensity was observed at 2.65 and 2.03 μm with almost equal intensities. The total specific radiation power at all wavelengths was 4 kW cm^{-3} at a pressure of 3 atm.

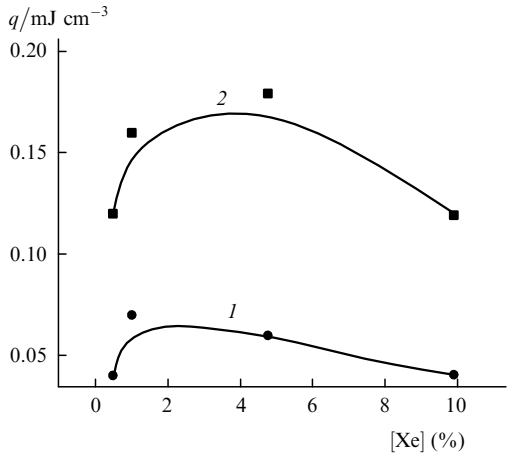

Figure 1. Dependences of the specific laser radiation energy q on the Xe concentration in (*1*) Ar–Xe and (*2*) Ar–Xe–N_2 mixtures at a 95-A cm^{-2} pump-current density and 2.5-atm mixture pressure measured on setup 2.

The results obtained on this setup are also presented in [5, 12].

Quasi-stationary lasing with a laser radiation pulse width of 30–100 μs was achieved on setup 3 at low beam-current densities. The maximum radiation energy in the Ar : Xe = 100 : 1 mixture was obtained at a pressure of 1 atm and a specific pump power of 1–3 kW cm^{-3}. As the pressure increased above 1 atm, a decrease in both the lasing efficiency and radiation energy was observed. When a broadband mirror was used, the 1.73-μm line made the main contribution to the lasing energy. On this setup, even small additions of molecular gases (the minimum measurable concentrations in our experiments were 0.05 %–0.1 %) resulted in a decrease in the radiation power and energy. Note that, as the pump power decreased, equal concentrations of molecular additions caused more significant decreases in the radiation energy and power. As the beam-current density increased and the pump current pulse was shortened to ~ 6 μs (the specific pump power at a pressure of 1 atm was ~ 6 kW cm^{-3}), N_2 additions gave no positive effect.

Setup 4 made it possible to perform investigations in the intermediate (compared to setups 2 and 3) beam-current duration and pump-power ranges. As was mentioned above, the highest positive effect of using molecular additions was observed on setup 2, whereas, on setup 3, adding molecular gases resulted in a decrease in the lasing power and energy. Figures 2–5 show the main dependences of the specific and total radiation energy as functions of the mixture composition and pressure, as well as the time-dependent lasing behaviour. Lasing arose with a delay of ~ 30 ns with respect to the beam-current pulse and terminated ~ 200 ns after the current pusle end. The main contribution to the lasing in the Ar–Xe mixture with the use of a broadband mirror was due to the 1.73-μm line. The maximum radiation energy was obtained at a 3.5-atm pressure in the Ar : Xe = 100 : 1 mixture and a specific pump energy input of ~ 56 mJ cm^{-3} (the specific pump power was ~ 140 kW cm^{-3}) (Fig. 2). However, a higher lasing efficiency was achieved at a mixture pressure of 2.5 atm (Figs 2 and 3a). Adding nitrogen to the working mixture in this setup resulted in both a decrease (at low energy inputs) and increase (at specific energy inputs of >30 mJ cm^{-3}) in the radiation energy.

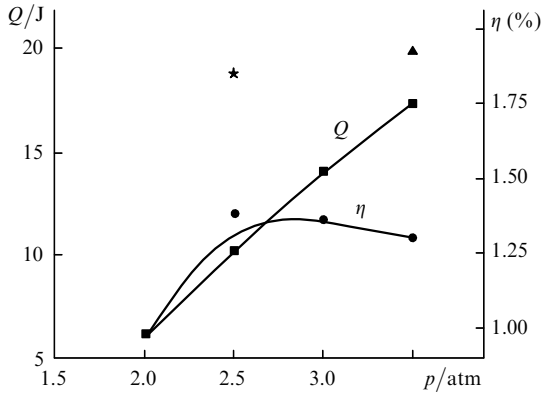

Figure 2. Lasing efficiency and radiation power Q versus pressure in the Ar–Xe mixture at a Xe partial pressure of 21 Torr obtained on setup 4 for specific energy inputs of 10–12 mJ cm^{-3} atm^{-1}: (★) maximum lasing efficiency for a specific energy input of 7.4 mJ cm^{-3} atm^{-1} and (▲) maximum lasing energy for a specific energy input of 16 mJ cm^{-3} atm^{-1}.

Figure 3 presents the specific radiation energy and lasing efficiency as functions of the specific pump energy for various mixtures, including those with nitrogen additions, at a pressure of 2.5 atm. This pressure was selected for comparison for two reasons. At this pressure, the maximum efficiencies were obtained in Ar–Xe mixtures, and, in addition, as the pressure increased above 2.5 atm, the

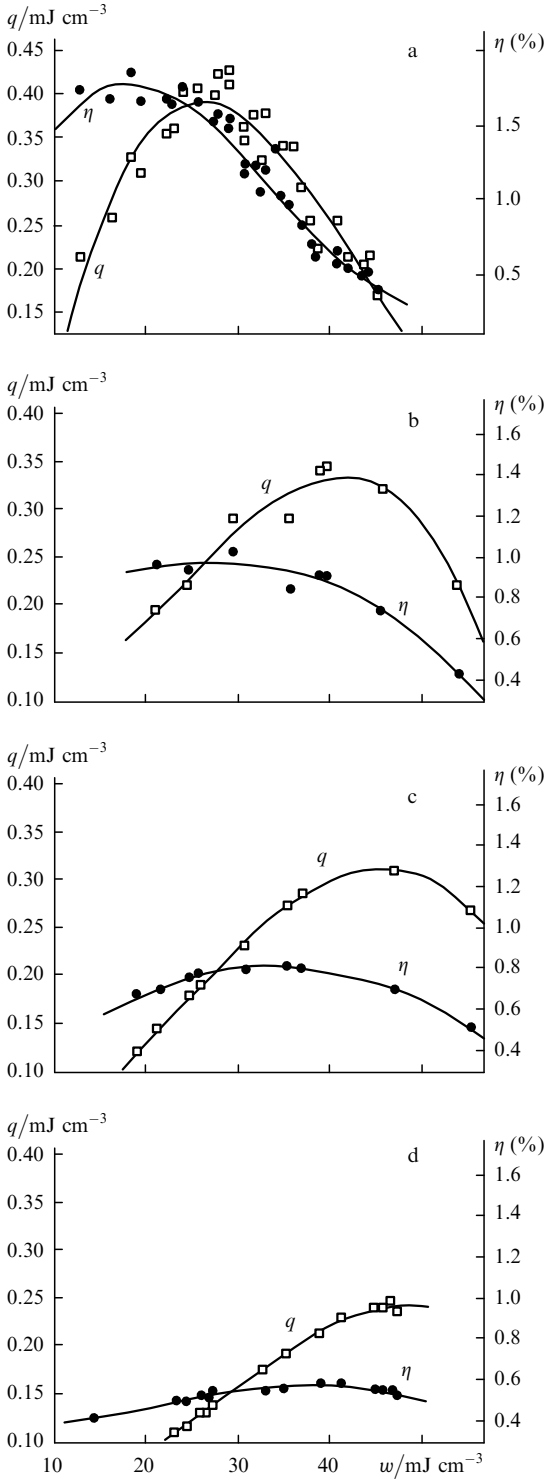

Figure 3. Specific radiation energy q and lasing efficiency η versus specific pump energy w at a pressure of 2.5 atm for (a) Ar : Xe = 100 : 1, (b) Ar : Xe : N_2 = 100 : 1.1 : 0.16, (c) Ar : Xe : N_2 = 100 : 1.1 : 0.4, and (d) Ar : Xe : N_2 = 100 : 1.1 : 0.64 mixtures.

uniformity of the excitation power distribution over the laser-chamber cross section degraded.

At a 2.5-atm pressure in an Ar–Xe mixture, the highest specific radiation energies (0.4–0.42 mJ cm^{-3}) were reached at a specific energy input of 25–30 mJ cm^{-3}, and, if the latter characteristic amounted to 40 mJ cm^{-3}, the specific radiation energy decreased to 0.22–0.25 mJ cm^{-3} (Fig. 3a). In a mixture with an optimal addition of nitrogen, the specific radiation energy was within 0.22 and 0.33 mJ cm^{-3} at a specific energy input of 20–25 and 40 mJ cm^{-3}, respectively (Fig. 3b). An increase in the N_2 concentration relative to the optimal one resulted in a shift of the maximum specific radiation energy to higher pump energy inputs, but the total and specific radiation energies and the lasing efficiency diminished in this case.

Figure 4 shows changes in the spectral composition of the radiation emitted by the Ar–Xe mixture with and without N_2 additions. The energy is predominantly emitted at 1.73 μm in both cases (Figs 4 and 5). The lasing energy at 2.63 μm is virtually independent on the energy input for both mixtures. The main differences in the radiation spectra manifest themselves in the fact that, in the presence of nitrogen, laser radiation at 3.37 and 3.51 μm is not observed, and the lasing energy at 2.65 μm abruptly increases, as the specific energy input increases above 35 mJ cm^{-3}. Nitrogen additions at equal energy inputs reduce the dip in the radiation pulse oscillogram at 1.73 μm. If argon was partially replaced by helium with

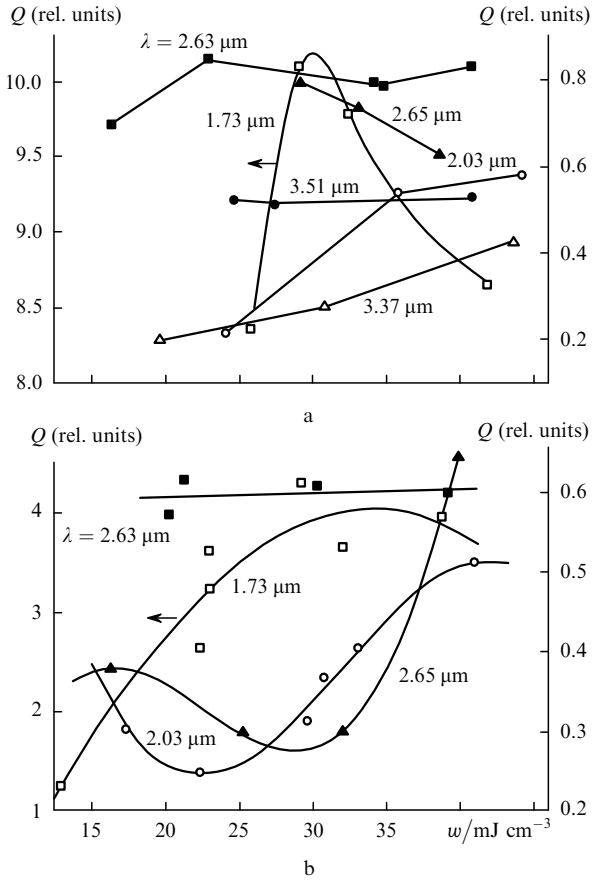

Figure 4. Lasing energy Q for various Xe atomic transitions in (a) Ar : Xe = 100 : 1.1 mixtures at a 2.5-atm pressure and in (b) Ar : Xe : N_2 = 100 : 1.4 : 0.4 mixtures at a 2.0-atm pressure versus specific pump energy averaged over the active volume (for setup 4).

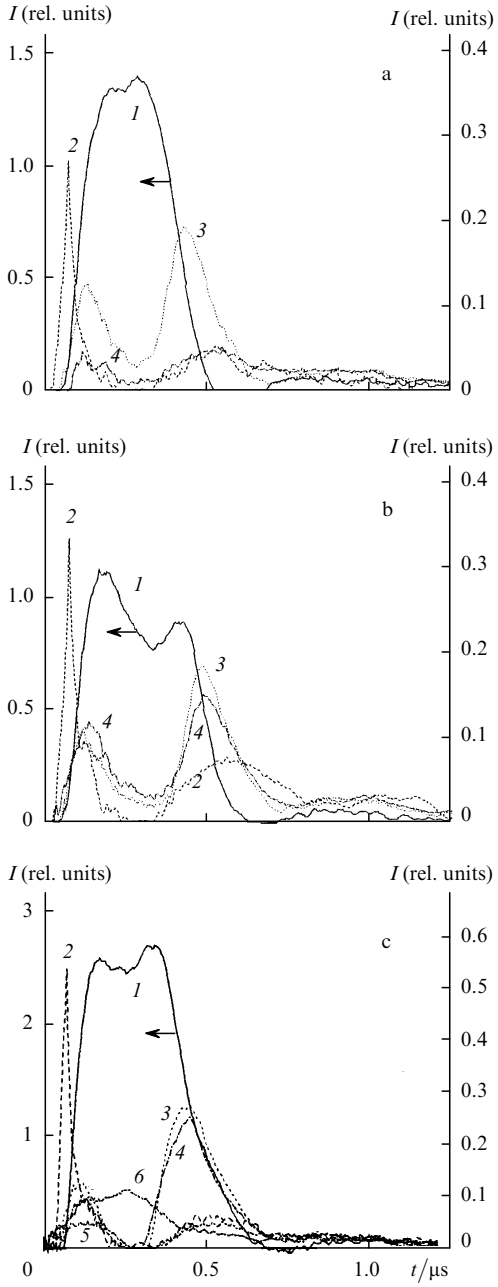

Figure 5. Oscillograms of laser pulses generated on Xe atomic transitions at λ = 1.73 (*1*), 2.03 (*2*), 2.63 (*3*), 2.65 (*4*), 3.37 (*5*), and 3.51 μm (*6*) in (a) Ar : Xe : N_2 = 100 : 1.4 : 0.4, (b) Ar : Xe : N_2 = 100 : 1.4 : 0.4, and (c) Ar : Xe = 100 : 1.1 mixtures at pressures of (a, b) 2.0 and (c) 2.5 atm and specific pump powers of (a) 29–31, (b) 38–40, and (c) ~32 mJ cm^{-3} (for setup 4).

a pressure in the mixture kept at 2.5 atm, a decrease in the specific radiation energy and lasing efficiency, compared to the parameters obtained in Ar–Xe and Ar–Xe–N_2 mixtures, was observed on setup 4.

4. Discussion

The basic processes leading to the pumping of the upper laser level in Ar–Xe mixtures have been studied well by now [16]. This is the recombination of molecular ions

$$ArXe^+ + e = Xe^* + Ar, \qquad (1)$$

$$Xe_2^+ + e = Xe^* + Xe, \quad (2)$$

excitation transfer from Ar^* to Xe

$$Ar^* + Xe = Xe^* + Ar, \quad (3)$$

a reaction of three-body recombination of Xe^+ ions

$$Xe^+ + e + e\,(He, Ar, Xe) = Xe^* + e\,(He, Ar, Xe) \quad (4)$$

and the process of excitation of Xe by electrons from the $6s$, $6s'$ states:

$$Xe(6s, 6s') + e \leftrightarrow Xe(5d) + e. \quad (5)$$

The rate constants of the these reactions are presented in [16]. Positive Xe ions are formed in the course of direct ionisation by secondary electrons during the charge exchange and due to the stepwise ionisation by plasma electrons, including the ionisation from the $6s$, $6s'$ states in the process

$$Xe(6s, 6s') + e = Xe^+ + 2e. \quad (6)$$

Quenching of the lower operating levels by argon and xenon atoms determines the inversion value at the laser transitions and the lasing spectrum.

The maximum radiation efficiencies ($\sim 4\,\%$) are realised in the Ar–Xe mixture at a pressure of ~ 1 atm and a specific pump power of $1-3$ kW cm^{-3} under quasi-stationary excitation by electron beams with durations of tens of microseconds. Similar results were obtained earlier in papers [9, 17, 18]. The maximum efficiency observed at a mixture pressure of 1 atm is determined by an optimal temperature of plasma electrons necessary for realising the channel for populating the upper laser level due to a stepwise excitation and ionisation [reactions (5) and (6)]. Under such conditions, especially with a decrease in the pump power, molecular additions lead to a decrease in the radiation energy and laser efficiency. Adding molecular gases or the presence of impurities causes a decrease in the electron temperature and reduces the contribution of reactions (5) and (6) to the pumping of the upper laser level.

At comparatively short beam pulse durations (tens of nanoseconds), an increase in the pump power is accompanied by a decrease in the lasing efficiency. However, in this case, the specific radiation power increased with increasing the specific pump power until the latter achieved the value of 1 MW cm^{-3}. We did not perform measurements at higher pump powers. A decrease in the lasing efficiency is caused by an increase in the electron concentration above an optimal one and, correspondingly, by a higher rate of mixing of laser levels by electrons. Under these conditions, an increase in the mixture pressure reduces the pump power per particle and the mixing of laser levels. This is accompanied by a decrease in the electron temperature, and a greater number of metastable Xe levels participate in the formation of molecules, so that the role of processes (5) and (6) becomes less significant. On the other hand, the contribution of ion recombination [mainly reaction (1)] to the population of the upper laser level increases. As a result, the radiation energy increases with the mixture pressure, but, according to the results of our measurements and data of other works [9, 17], the lasing efficiency decreases. Molecular additions reduce the electron concentration, giving a positive effect due to a decrease in the mixing of laser levels, and cool electrons, leading to an increase in the recombination rate and, probably, in the rate of depopulation of the lower laser level [5]. For a beam duration of several tens of nanoseconds, a maximum increase in the radiation power and energy due to molecular additions is observed.

For a nanosecond high-density electron beam (only an afterglow lasing is observed), molecular additions also accelerate the cooling of electrons (the recombination rate increases) and reduce their concentration (the mixing of laser levels decreases). However, electrons are cooled in the afterglow at a higher rate than during the beam action, and the relative increase in the radiation energy with molecular additions is lower than for beam durations of tens of nanoseconds, and this energy increase is virtually absent with an increase in the mixture pressure.

As the beam-current pulse duration increases up to several hundreds of nanoseconds, the highest radiation energies are reached (all factors being the same) at optimal beam-current densities and presures of $2-5$ atm. At optimal pump powers, the highest lasing efficiency are achieved, and molecular additions reduce the radiation energy. However, if the pump power and beam-current density increase [in wide-aperture setups, this is achieved by increasing the charging voltage of a pulse generator, which results in a simultaneous increase in the voltage across the VD (i.e., in the electron energy)] at a constant pressure, the lasing efficiency decreases and, at higher pump powers, a similar behavior is observed for the radiation energy (Fig. 3a). A positive effect of molecular additions at increased energy inputs consists not only in an enhanced radiation energy and lasing efficiency but also in a more uniform distribution of the radiation power density over the cross section of the output laser beam. This is achieved through an increase in the electron energy at elevated charging voltages.

Note that, when a discharge initiated or controlled by an electron beam is used to pump an active medium, an electric field makes it possible to increase the electron energy. At an elevated pressure ($3-5$ atm) in the Ar–Xe mixture, this ensured an optimal electron temperature for exciting and ionising metastable Xe levels [processes (5) and (6)] and the obtainment of a lasing efficiency of $\sim 4\,\%$ (with respect to the energy stored in the capacitive storage) at a pressure of several atmospheres [2, 4, 10]. Electron cooling through collisions with molecular additions under such conditions reduces the radiation energy and lasing efficiency.

5. Conclusions

The experimental studies of a Xe atomic transition laser performed within broad ranges of working mixtures, pressures, and durations and specific powers of the pump electron beam allowed us to determine the conditions under which molecular gas additions in the Ar–Xe mixture improve the laser output characteristics. The factors affecting the Xe laser efficiency were analysed. It was confirmed that the maximum efficiencies of the Ar–Xe laser are realised when stepwise excitation and ionisation of metastable Xe levels participate in populating the upper laser level.

An increase in the specific energy input to the Xe-laser working medium above an optimal level first leads to a reduction of the lasing efficiency and, as the specific pump

power continues to rise, the above effect is accompanied by a decrease in the output radiation power. When short laser pulses (tens of nanoseconds) are generated, the output power of the Xe atomic transition laser, the radiation energy, and lasing efficiency can be increased by adding molecular gases (N_2 and CO_2) at low concentrations to the working medium. For pump pulse durations of 100 ns and longer, an overexcitation of the working medium results in a dip in the laser pulse at maximum beam-current densities, and an addition of a molecular gas or helium reduces or cancels this dip. Low-concentration (a few percent) impurities of molecular gases have virtually no effect on the working-medium pressure, which is usually selected to be as high as possible at high pump powers, and allow one to increase the radiation power and energy at pump powers above 40 kW cm^{-3} atm^{-1}. However, a further increase in the laser radiation energy is achieved by maintaining the specific pump energy input and increasing the Ar–Xe mixture pressure.

Acknowledgements. This work was supported by the International Science and Technology Center (Grant No. 1206).

References

1. Lawton S.A., Richards J.B., Newman L.A., Spech L., De Temple T.A. *J. Appl. Phys.*, **50**, 3888 (1979).
2. Losev V.F., Tarasenko V.F. *Kvantovaya Elektron.*, **7**, 663 (1980) [*Sov. J. Quantum Electron.*, **10**, 381 (1980)].
3. Bychkov Yu.I., Losev V.F., Tarasenko V.F., Tel'minov E.N. *Pis'ma Zh. Tekh. Fiz.*, **8**, 837 (1982).
4. Basov N.G., Danilychev V.A., Dudin A.Yu., Zayarnyi D.A., Ustinovskii N.N., Kholin I.V., Chugunov A.Yu. *Kvantovaya Elektron.*, **11**, 1722 (1984) [*Sov. J. Quantum Electron.*, **14**, 1158 (1984)].
5. Bunkin F.V., Derzhiev V.I., Mesyats G.A., Skakun V.S., Tarasenko V.F., Yakovlenko S.I. *Kvantovaya Elektron.*, **12**, 874 (1985) [*Sov. J. Quantum Electron.*, **15**, 575 (1985)].
6. Basov N.G., Baranov V.V., Danilychev V.A., Dudin A.Yu., Zayarnyi D.A., Rzhevskii A.V., Ustinovskii N.N., Kholin I.V., Chugunov A.Yu. *Kvantovaya Elektron.*, **13**, 1543 (1986) [*Sov. J. Quantum Electron.*, **16**, 1008 (1986)].
7. Koval' N.N., Kreindel' Yu.E., Mesyats G.A., Skakun V.S., Tarasenko V.F., Tolkachev V.S., Fedenev A.V., Chagin A.A., Shchanin P.M. *Pis'ma Zh. Tekh. Fiz.*, **12**, 37 (1986).
8. Derzhiev V.I., Koval' N.N., Mesyats G.A., Prokhorov A.M., Skakun V.S., Tarasenko V.F., Tolkachev V.S., Fomin E.A., Yakovlenko S.I. *Kvantovaya Elektron.*, **14**, 427 (1987) [*Sov. J. Quantum Electron.*, **17**, 269 (1987)].
9. Watterson R.L., Jacob J.H. *IEEE J. Quantum Electron.*, **26**, 417 (1990).
10. Suda A., Wexler B.L., Riley K.J., Fildman B.J. *IEEE J. Quantum Electron.*, **26**, 911 (1990).
11. Litzenberger L.N., Trainor D.W., McGeoch M.W. *IEEE J. Quantum Electron.*, **26**, 1668 (1990).
12. Skakun V.S., Tarasenko V.F., Fedenev A.V. *Opt. Spekrosk.*, **71**, 669 (1991).
13. Sereda O.V., Tarasenko V.F., Fedenev A.V., Yakovlenko S.I. *Kvantovaya Elektron.*, **20**, 535 (1993) [*Quantum Electron.*, **23**, 459 (1993)].
14. Bugaev A.S., Koval N.N., Lomaev M.I., Mel'chenko S.V., Ryzhov V.V., Tarasenko V.F., Turchanovsky I.Yu., Fedenev A.V., Shchanin P.M. *Laser and Particle Beams*, **12**, 6 4, 633 (1994).
15. Patterson E.L., Samlin G.E. *J. Appl. Phys.*, **76**, 2582 (1994).
16. Karelin A.V., Sinyanskii A.A., Yakovlenko S.I. *Kvantovaya Elektron.*, **24**, 387 (1997) [*Quantum Electron.*, **27**, 375 (1997)].
17. Zayarnyi D.A., Semenova L.V., Ustinovskii N.N., Kholin I.V., Chugunov A.Yu. *Kvantovaya Elektron.*, **25**, 493 (1998) [*Quantum Electron.*, **28**, 478 (1998)].
18. Tarasenko V.F., Fedenev A.V., Skakun V.S. *Kvantovaya Elektron.*, **26**, 209 (1999) [*Quantum Electron.*, **29**, 209 (1999)].
19. Karelin A.V., Simakov O.V. *Kvantovaya Elektron.*, **28**, 121 (1999) [*Quantum Electron.*, **29**, 678 (1999)].
20. Fedenev A.V., Karelin A.V., Simakova O.V., Tarasenko V.F. *Proc. SPIE Int. Soc. Opt. Eng.*, **4747**, 137 (2002).
21. Abdillin E.N., Gorbachev S.I., Efremov A.I., Koval'chuk B.M., Loginov S.V., Skakun V.S., Tarasenko V.F., Tolkachev V.S., Fedenev A.V., Fomin E.A., Shchanin P.M. *Kvantovaya Elektron.*, **20**, 652 (1993) [*Quantum Electron.*, **23**, 564 (1993)].